journal

J. Am. Ceram. Soc., 74 [2] 255–69 (1991)

Microstructural Design of Toughened Ceramics

Paul F. Becher*

Metals and Ceramics Division, Oak Ridge National Laboratory, Oak Ridge, Tennessee 37831-6068

The fracture toughness of ceramics can be improved by the incorporation of a variety of discontinuous, elastic reinforcing phases that generate a crack-bridging zone. Recent models of toughening by crack-bridging processes are discussed and used to describe the behavior observed in whisker-reinforced ceramics. The toughening response in ceramics reinforced with other types of discontinuous reinforcements is then considered (e.g., matrix and second-phase platelike grains, elongated matrix grains, and grain-size effects in noncubic matrices). It is shown that crack-bridging toughening processes can be combined with other bridging mechanisms and with other toughening mechanisms (e.g., transformation toughening) to achieve synergistic effects. From these discussions, it is shown that the design of the toughened materials relies heavily on the control of the material properties and microstructural components influencing the toughening behavior to optimize the contributions of both the reinforcing phase and the matrix. [Key words: toughness, microstructure, bridging, reinforcement, transformation toughening.]

S. M. Wiederhorn—contributing editor

Manuscript No. 197225. Received October 12, 1990; approved November 26, 1990.

Presented at the 92nd Annual Meeting of the American Ceramic Society, Dallas, TX, April 26, 1990 (Robert Browning Sosman Lecture).

Supported by the Division of Materials Sciences, U.S. Department of Energy, under Contract No. DE-AC05-84OR21400 with Martin Marietta Energy Systems, Inc.

*Member, American Ceramic Society.

I. Introduction

THE brittle nature of ceramics has, over the years, prompted us to explore a variety of approaches to enhance their fracture toughness/resistance. Normally, the fracture of brittle materials involves very little dissipation of the applied strain energy by processes other than extension of the crack. In extremely brittle systems, the fracture surface energy, γ_{IC}, often approaches the surface free energy. In glasses and single crystals, the related fracture toughness ($K_{IC}=(2\gamma_{IC}E)^{1/2}$, where E is Young's modulus of the material) can be extremely low (e.g., 0.5 to 2 MPa·m$^{1/2}$)[1a] as compared with metals (15 to 150 MPa·m$^{1/2}$).[1b] Even in polycrystalline ceramics, including a wide variety of oxides and non-oxides, the fracture toughness values are ≤5 MPa·m$^{1/2}$. Until recent years, the success in improving the fracture toughness of ceramics had been limited to a few specific cases (e.g., cobalt-bonded tungsten carbides). However, within the last decade, numerous approaches to improve the fracture toughness of ceramics have been developed as noted later in this section.

On the other hand, very high flexure strengths can be achieved in ceramics, even with their low fracture resistance, by very stringent processing procedures.[2] High strengths can now be achieved even in large-sized components. However, the processing requirements are quite strict as compared with those for more fracture resistant materials. Using the Griffith relationship,[3] we note that strengths of 800 MPa require that crack sizes must be less than 25 μm for simple semicircular surface cracks if the toughness is only 5 MPa·m$^{1/2}$. This extreme in the flaw-size sensitivity of the fracture

strength combined with variations in flaw size yields very broad strength distributions (i.e., low Weibull moduli). As a result, designers of ceramic components have actively sought to eliminate or greatly minimize tensile stresses in service. This has meant that we could take advantage of only a small fraction of potential tensile/flexure strengths. Today, progress in the processing of ceramics, in the machining of ceramics, and in nondestructive evaluation is providing us with the ability to produce ceramic components with both much-improved fracture strengths and narrow strength distributions.

Despite these particular advances, low-toughness ceramics are subject to loss of a substantial fraction of their strength because of damage introduced during service (e.g., because of static load slow crack growth, cyclic fatigue, creep damage, thermal gradients and/or shock, and impact or contact damage). Thus, material design approaches that can impart a substantial degree of toughness to ceramics obviously can have a significant impact in minimizing both strength distributions (increasing Weibull moduli) and losses due to in-service damage and crack growth. This is shown in the examples of improved mechanical performance achieved in alumina composites illustrated in Table I. Table I also shows that not only is there a much lower scatter in room-temperature strengths, but that the high strength and fracture toughness are maintained to elevated temperatures. Furthermore, the toughened aluminas have much greater resistances to thermal-shock damage, the onset of slow crack-growth damage, and tension–tension cyclic fatigue.

Table I. Properties of Reinforced Alumina Ceramics

Fine-Grained Al_2O_3 + 20 vol% SiC Whiskers

Temperature (°C)	Fracture toughness (MPa·m$^{1/2}$)	Four-point flexure strength, σ_f (MPa)
22	8–9	650–800
1000	8	575–775
1200	10	475–550

Alumina versus Composite Thermal Shock Resistance

Temperature change, ΔT (°C)	Retained strength (MPa)*	
	Alumina	Alumina + 20 vol% SiC whiskers
300	300	650
500	200	
700	80	650
900		700

Slow Crack-Growth Resistance

Applied stress intensity (MPa·m$^{1/2}$)	log (crack velocity) (m/s)†	
	Alumina	Alumina + 20 vol% SiC whiskers
4.0	−7.2	
4.4	−3.1	
8.0	>>−3	−7.2
8.8	>>−3	−3.1

Strength

	Flexure strength (MPa)‡	Weibull modulus‡
Alumina	530	4.6
Alumina + ~19 vol% SiC whiskers	600	13.4

Tensile Cyclic Fatigue

	Peak stress	Cycles to failure§
Alumina	315	1
	250	6×10^2
	210	7×10^5
Alumina + 35 vol% SiC whiskers	435	1
	330	1.1×10^5 (NF)¶
	+367	4×10^4 (NF)
	+396	3×10^4 (NF)
	+414	6×10^2

*Quenched into 100°C water. †Slow crack-growth resistance in air at 20°C. ‡Room temperature (Ref. 4). §20°C (Ref. 5). ¶NF means sample did not fail; test continued at higher peak stress. Minimum stress was 10% of peak stress.

Improvements in these particular mechanical properties combined with the potential for long service life have prompted the research community to search for mechanisms which impart increased fracture toughness/resistance to ceramics. A number of approaches have been devised which can yield ceramics with fracture-toughness values as high as 10 to 20 MPa·m$^{1/2}$. Among the mechanisms that can contribute to such significant improvements in fracture toughness are crack pinning,[6] crack deflection,[7] crack bridging, and pullout[8,9] by dispersed particles and elastic-reinforcing phases and grains, and/or stress-induced microcracking.[10] Stress-induced martensitic transformation toughening[11] in monolithic zirconias and systems containing dispersed zirconia particles and plasticity in metallic binder (e.g., cobalt-bonded tungsten carbides) and dispersed phases[12] also enhance fracture resistance. The magnitude of the improvements in the fracture toughness obtained in selected ceramics is illustrated in Table II.

In this paper, the processes leading to improvements in the fracture resistance of ceramics containing discontinuous elastic reinforcing phases are reviewed. The increased fracture toughness for whisker-reinforced composites is discussed in terms of crack-bridging processes and in the context of crack-bridging micromechanics models. The bridging models provide a very useful means to illustrate how the properties of the matrix, interface, and reinforcing phase characteristics influence the fracture resistance of the composite. The applicability of crack-bridging processes is extended to consider other approaches that can lead to increased toughness. Those processes considered here include crack bridging by other types of second phases (platelets) and by matrix grains. Finally, the potential toughening response achieved by combined or coupled toughening processes is char-

acterized, and examples are given which illustrate the substantial effects that can be derived in this way.

II. Toughening by Crack Bridging

Very substantial toughening effects (at least threefold to fivefold increases in fracture toughness) can be achieved through the judicious use of discontinuous, elastic second phases. The toughening results from bridging of the crack surfaces behind the crack tip by a strong reinforcing phase that imposes a closure force on the crack. This crack-bridging toughening process is often supplemented by a contribution due to pullout of the reinforcement.[9,13–16] The extent of pullout (i.e., the pullout length) in the case of discontinuous, elastic reinforcing phases may be quite limited (e.g. whisker reinforcement) because of both the short length of such phases and the fact that the extent of the interfacial bonding and the magnitude of the interfacial clamping stresses can minimize pullout. However, pullout cannot be ignored because even short pullout lengths will contribute to the toughness achieved, as we shall show later. Crack deflection by such reinforcements has also been suggested to contribute to the fracture resistance. Often, out-of-plane (other than Mode I) crack deflections are limited in distance and angle as they progress away from the original Mode I crack-plane projection. In the case of fine-grained (1 to 2 μm) alumina reinforced with whiskers, crack deflections are on the scale of the grain size. Instead, crack deflection in many of these systems is associated with a reinforcement–matrix interface-debonding process. Such interfacial debonding is important in achieving both crack bridging (bridging by elastic ligaments that are partially debonded from the matrix) and subsequent pullout of the reinforcing phase.

As we will show, elastic bridging ligaments (e.g., whiskers, platelets, grains) contribute significantly to the fracture toughness, as does pullout (e.g., matrix grain bridging, whisker pullout). In the next section we will first concentrate on crack bridging as a toughening process and the parameters affecting the magnitude of the toughening contribution and then similarly address the pullout contribution citing the observations on whisker-reinforced ceramics. Then we will consider how these toughening processes can be extended to other types of reinforcements to obtain similar toughening behavior.

(1) Analysis of Toughening by Discontinuous Elastic Reinforcements

We consider now the toughening contribution due to crack bridging by various elastic reinforcing phases where the reinforcement is partially debonded and bridges the crack surfaces. This process effectively pins the crack surfaces together, thereby increasing the resistance to crack extension. In an earlier paper[9] the toughening response for whisker-reinforced ceramics was described by characterizing the stress-intensity difference associated with a bridging zone of a given length. Here we consider the energy dissipation by bridging processes; note that the results are quite similar. In the present discussion we address crack bridging (elastic and frictional) associated with partially debonded reinforcements as well as pullout of the reinforcements. Based on the energy dissipation/energy balance approach, the crack-bridging contribution to the toughness is

$$K_{IC}^{c}=[E^{c}(J^{m}+\Delta J^{cb})]^{1/2}=(E^{c}J^{c})^{1/2} \quad (1a)$$

$$K_{IC}^{m}=(E^{m}J^{m})^{1/2} \quad (1b)$$

where K_{IC}^{c} is the overall toughness of the composite and E^{c} is Young's modulus of the composite. Here we use the terms ΔJ^{cb} and J^{m} to define energy change associated with the bridging process and with crack extension in the matrix, respectively. These quantities are determined using the J-integral approach. The J^{m} term is the sum of terms J^{o}, the component due to bond rupture in the matrix, and ΔJ^{m}, the contribution of other matrix terms (discussed later). In the case of glasses and elastic cleavage of single crystals, $J^{m}=J^{o}$, which is equal to $2\gamma^{o}$, the intrinsic fracture surface energy.

Table II. Fracture Toughness Values for Various Ceramic Materials*

Material†	G (μm)‡	Fracture toughness (MPa·m$^{1/2}$)
Alumina	1–2	2.5–3
	10–12	4.5
Alumina + 20 vol% SiC whiskers	1–2	8–10
Alumina + 20 vol% TZP (1 mol% yttria)§	2	8
Alumina + 40 vol% TZP (12 mol% ceria)§	2	13
Polycrystalline cubic zirconia	~50	3
TZP (12 mol% ceria)§	4–6	15–18
TZP (2 mol% yttria)§	1.5	12
TZP (2 mol% yttria)§	0.5	7
PSZ (9 mol% magnesia) with increasing precipitate size§	50	8–16
Silicon nitride, equiaxed grains	2–3	4
Silicon nitride, elongated grains	~4¶	10
Silicon carbide, densification additive—alumina	2	3.5–4.0
Silicon carbide, densification additive—boron and carbon	5–7	2.5–3.0
Silicon carbide + 25 vol% titanium carbide	2.5	6

*Values determined at room temperature in author's laboratory using precracked (3- to 5-mm precrack length) applied-moment double-cantilever-beam specimen. †TZP is polycrystalline tetragonal zirconia, PSZ is partially stabilized zirconia. ‡G represents average grain size of equiaxed polycrystalline matrix phase. §Toughness values are quite sensitive to test temperature. ¶Diameter of grain.

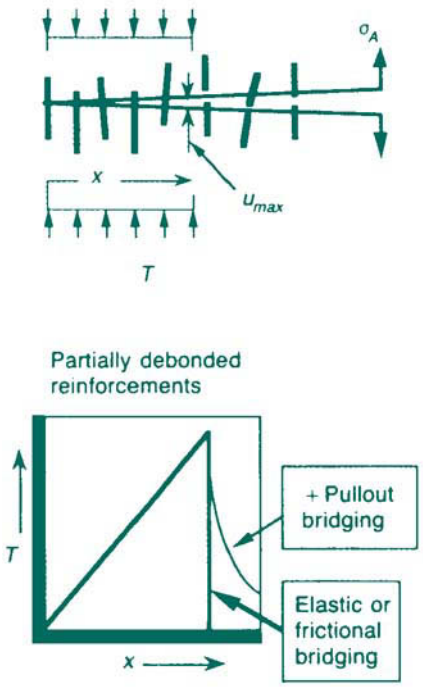

Fig. 1. Crack bridging by discontinuous brittle reinforcing phases imposes a closure or bridging stress in the wake of the crack tip and enhances the fracture resistance of the brittle matrix.

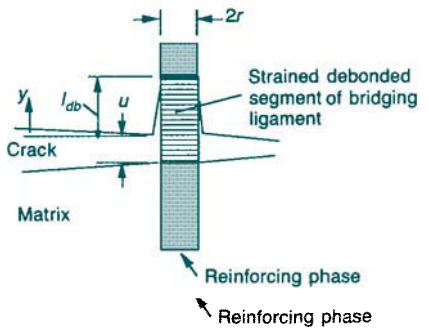

Fig. 2. Crack-opening displacement associated with the bridging zone is related to the tensile displacement in elastic bridging ligaments in the absence of interfacial friction. At the end of the bridging zone, the maximum crack opening is equivalent to the displacement in the ligament corresponding to its fracture stress.

(A) Bridging by Partially Debonded Reinforcement: The energy change associated with the bridging process can be shown to be a function of the bridging stress/traction, T_u, and the crack-opening displacement, u, and is defined as

$$\Delta J^{cb} = \int_0^{u_{max}} T_u \, du \tag{2}$$

where u_{max} is the displacement at the end of the zone[17] (Fig. 1). If the reinforcement–matrix interface does not debond and the crack front moves past the reinforcement, the crack-opening displacement will be limited by the elastic displacement in the reinforcement across the crack surfaces. In the absence of interfacial debonding, this is extremely small and is limited by Young's modulus of the reinforcement (the smaller the Young's modulus of the reinforcement the greater the displacement). The lack of debonding also causes the stress imposed on the reinforcement to reach its fracture strength immediately behind the crack tip, where u is extremely small. Even with ultra-high-strength reinforcements, the toughening effects are small.

When interfacial debonding occurs, the stress and resultant strain imposed on the bridging reinforcement is no longer localized to the region between the main crack surfaces. As a result, greater crack-opening displacements are achieved within the bridging zone, yielding larger toughening effects. When there is no interfacial friction and the bridging stress increases linearly from zero at the crack tip to a maximum at the end of the bridging zone (and immediately decreases to zero, see Fig. 1), Eq. (2) can be simplified to $T_{max}u_{max}/2$. For the simplest case, the maximum closure stress, T_{max}, imposed by the reinforcing ligaments in the crack-tip wake, is the product of the fracture strength of the ligaments, σ_f^l and the areal fraction of ligaments intercepting the crack plane, A^{el}:

$$T_{max} = \sigma_f^l A^{el} \cong \sigma_f^l V^{el} \tag{3}$$

where A^{el} can be approximated by the volume fraction, V^{el}, for ligaments that have large aspect ratios (e.g., $l/r \geq 30$ for whiskers). For a composite where the reinforcements are uniaxially aligned normal to the crack plane, V^{el} will equal the volume fraction of reinforcements added. For most reinforced composites, the reinforcing phase exhibits some degree of random orientation. There is no model at present to deal satisfactorily with this phenomenon. Instead, we must use experimental observations to determine the fraction of reinforcements contributing to the crack-bridging and pullout processes. Although this may cause some concern, the fact that the reinforcements have some degree of random orientation means that the mechanical properties will be less variable with regard to orientation of the stress axis.

In the case of partially debonded bridging ligaments, the maximum crack-opening displacement at the end of the bridging zone, u_{max}, is equivalent to the tensile displacement within the debonded section of the ligament spanning the crack at this point. This means that the maximum crack opening

$$u_{max} = \epsilon_f^l l_{db} \tag{4}$$

is limited by the strain to failure of the ligament, ϵ_f^l, and the debonded length of the matrix–ligament interface, l_{db} (Fig. 2). The strain to failure of the partially debonded ligament,

$$\epsilon_f^l = \sigma_f^l / E^l \tag{5}$$

is a function of the strength, σ_f^l, and Young's modulus of the reinforcing phase, E^l. Next, the interfacial debond length can be shown to depend on the fracture criteria for the reinforcing phase versus that of the interface and can be defined in terms of either fracture stress or fracture energy. The analysis of Budiansky *et al.*[18] defines the critical debond length for debonding initiated just ahead of the main crack tip as

$$l_{db} = r\gamma^l / 6\gamma^i \tag{6}$$

where γ^l/γ^i represents the ratio of the fracture energy of the bridging ligament to that of the reinforcement–matrix interface, and r is the radius of the bridging ligament. This definition of the debond length likely describes only the initial debond length. If the interfacial failure criterion (fracture energy or stress) is relatively low, we would not be surprised to see the interfacial cracks grow (Mode II) because of stresses on the bridging reinforcements in the crack-tip wake. Evidence for interfacial debonding is noted in Fig. 3, where debonding of SiC-whisker interfaces is observed.

In the absence of interfacial friction, crack bridging by the elastic "stretching" of bridging ligaments which are partially debonded then dissipates energy to the extent

$$\Delta J^{eb} = \frac{A^{el}(\sigma_f^l)^2}{2E^l} l_{db} \tag{7}$$

where l_{db} is defined by $r\gamma^l/6\gamma^i$.

Again, the previous analysis considered that there is no interfacial frictional interaction between the partially debonded reinforcement and the matrix. This would be appropriate, for example, when the thermal-expansion coefficient of the matrix, α_m, is less

than that of reinforcing phase, α_i.

When frictional forces are imposed along the debonded interface, e.g., $\alpha_m > \alpha_i$, the previous analysis must be modified as noted in Refs. 7(c), 7(d), and 9. Here we address the case where the frictional shear resistance, τ_i, is constant along the partially debonded interface. The stress on the partially debonded whisker is no longer constant along its length (debonding per Fig. 2) but decays from a maximum at the point where the reinforcement exits the crack surface ($y=0$) to zero at the end of the debond ($y=l_{db}$). Thus, the stress in the reinforcement is

$$\sigma_y^I = \frac{2(l_{db}-y)\tau_i}{r} \tag{8a}$$

and has a maximum value of

$$\sigma_y^I = \frac{2l_{db}\tau_i}{r} \tag{8b}$$

at $y=0$, the crack surface. Consequently, the tensile displacement in the bridging reinforcement and the crack-opening displacement, u (Eqs. (4) and (5)), are altered:

$$u = \frac{l_{db}^2\tau_i}{E^I r} = \frac{r\sigma_y^2}{4E^I\tau_i} \tag{9a}$$

$$u_{max} = \frac{r(\sigma_f^I)^2}{4E^I\tau_i} = \frac{E_f^I}{2} l_{db} \tag{9b}$$

The term u_{max} can also be obtained by integrating over the range of stress acting on the whisker:

$$u_{max} = \frac{r}{4E^I\tau_i}\int_0^{\sigma_f^I} 2\sigma_y \, d\sigma_u = \frac{r(\sigma_f^I)^2}{4E^I\tau_i} \tag{9c}$$

For the case of elastic stretching of a partially debonded reinforcement subject to interfacial friction (τ_i is constant), the energy consumption is

$$\Delta J^{fb} = A^{fb}\int_0^{u_{max}} \sigma_y \, du = \frac{A^{fb}r}{4E^I\tau_i}\int_0^{\sigma_f^I} 2\sigma_y^2 \, d\sigma_u \tag{10a}$$

where the expression for du is obtained from Eq. (9a), which yields

$$\Delta J^{fb} = \frac{A^{fb}r(\sigma_f^I)^3}{6E^I\tau_i} = \frac{A^{fb}(\sigma_f^I)^2 l_{db}}{3E^I} \tag{10b}$$

where again A^{fb} can be approximated by V^{fb} for long, aligned reinforcements.

From Eqs. (4) and (9b), we note that the tensile strain displacement achieved in the bridging reinforcement and, hence, the maximum crack-opening displacement at the end of the bridging zone increase as the debonded length or gauge length of the reinforcing ligament increases. Consideration of Eqs. (5), (6), and (8b) illustrates the importance of increasing the reinforcing phase strength and/or enhancing interface debonding to achieve greater tensile displacement within the reinforcing ligament. Ultimately, we can show from Eq. (2) (or the specific forms, Eqs. (7) and (10)) that increases in the crack-opening displacement supported by the bridging zone will enhance the fracture resistance achieved by such reinforcements, again emphasizing the importance of interfacial debonding in the toughening response.

The resultant fracture toughness of a composite due to elastic stretching of a partially debonded reinforcing phase in the crack-tip wake with no interfacial friction is

$$K^c = \left[E^c J^m + (\sigma_f^I)^2 \frac{rV^{el}E^c\gamma^I}{12E^I\gamma^i}\right]^{1/2} \tag{11a}$$

where l_{db} is described by $r\gamma^I/6\gamma^i$.[18] When elastic stretching of a partially debonded reinforcement includes a frictional component at the interfaces, the toughness becomes

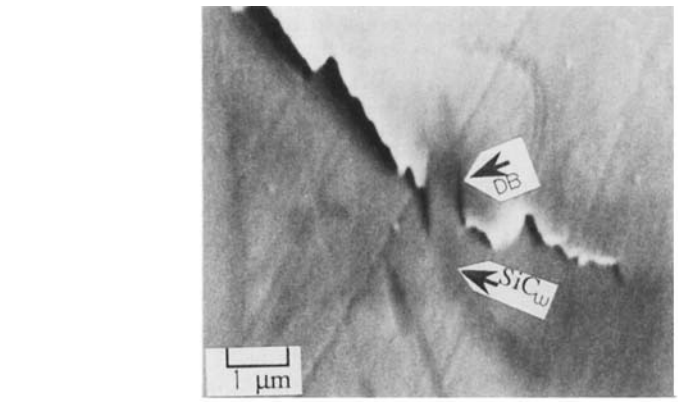

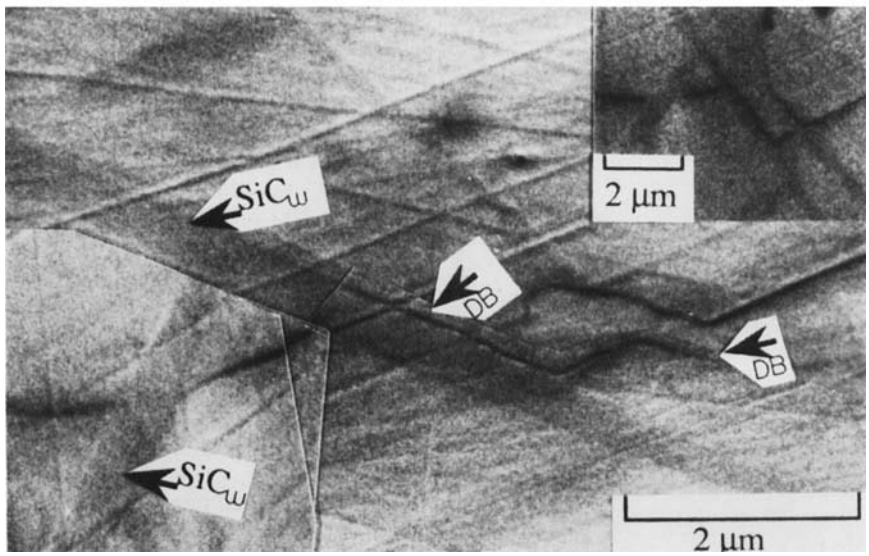

Fig. 3. Debonded whisker–matrix interfaces are associated with whisker bridging in the region immediately behind the crack tip in a polycrystalline alumina matrix. Images obtained by scanning electron microscopy of flexure bar containing indentation cracks propagated in four-point loading.

$$K^c=\left[E^cJ^m+(\sigma_f^l)^2\frac{rV^{fb}E^c}{6E^l}\frac{\sigma_f^l}{\tau_i}\right]^{1/2} \quad (11b)$$

where l_{db} now equals $r\sigma_f^l/2\tau_i$. The overall toughness of the composite then includes both the specific bridging contribution from the reinforcing phase (Eqs. (7) and (10*b*)) and the fracture resistance of the matrix per discussion of Eq. (1). As Eqs. (11*a*) and (11*b*) imply, all the parameters contributing to the toughness must be accounted for and taken advantage of in the development of toughened ceramics and composites. For example, we cannot assume that every whisker will provide significant toughening effect or that the same whisker will work equally well in all matrices, as reflected by the need to control the diameter and strength of the whiskers.

(B) Pullout: When pullout accompanies frictional bridging, additional strain energy must be supplied to advance the crack. The energy consumption due to pullout is determined using Eq. (2) as a starting point. The crack opening associated with pullout is equal to u'_{max} (at the point behind the crack tip where the reinforcement is totally extracted from the matrix) minus u_{max} (the crack opening at the end of the frictional bridging zone). However, for most observations of discontinuous reinforcements, $u'_{max}\gg u_{max}$. The declining pullout bridging stress with increase in crack opening (Fig. 1) can be described as

$$T_u=T_{max}(1-u/u'_{max}) \quad (12)$$

with the proviso that $u'_{max}-u_{max}$ approaches u'_{max}. The maximum bridging stress ($T_{max}=A^{po}\sigma_y^l$) is a function of the interfacial frictional shear resistance defined in Eq. (8*b*). σ_y^l has a peak value at the point where the reinforcement exits the crack surface ($y=0$, Fig. 2). To obtain pullout, the reinforcement must fracture at a position $y>0$. The pullout length l_{po}, is then generally less than l_{db} and is a function of the defects and stress concentrations in the reinforcing ligament. The axial stress due to reinforcement pullout is

$$\sigma_y^{po}=\frac{2\tau_i}{r}l_{po} \quad (13)$$

Assuming a linear decay in the pullout stress–displacement response and substituting Eq. (13) into Eqs. (12) and (2), the pullout contribution to the energy consumption process is

$$\Delta J^{po}=A^{po}\tau_i\left(\frac{l_{po}}{r}\right)l_{po}=A^{po}\tau_i\, r\left(\frac{l_{po}}{r}\right)^2 \quad (14a)$$

$$\Delta K^{po}=(E^cA^{po}\tau_i\, r)^{1/2}l_{po}/r \quad (14b)$$

where A^{po} represents the areal fraction of pullouts and $l_{po}\propto r\sigma_f^l/2\tau_i$. Again, for reinforcing phases with large aspect ratios, the volume fraction of pullouts, V^{po}, closely approximates A^{po}.

Using Eqs. (14*a*) and (10*b*), we can determine the relative contributions obtained from pullout versus that from frictional bridging:

$$\frac{\Delta J^{po}}{\Delta J^{fb}}=3\frac{l_{po}}{r}\frac{\tau_i E^l}{(\sigma_f^l)^2}\frac{V^{po}l_{po}}{V^{fb}l_{db}} \quad (15)$$

where the ratios l_{po}/r, l_{po}/l_{db}, and V^{po}/V^{fbl} have strong influences.

(2) Toughening Response with Bridging Whiskers

Before proceeding further, let us examine an example of the toughening response in ceramics reinforced with discontinuous elastic SiC whiskers. In SiC-whisker-reinforced alumina, the observed upper limit value of l_{po}/r is ~4, and the calculated value of τ_i ($=\mu\sigma_r$, where μ is the coefficient of friction (~0.25) and σ_r is the radial thermal-expansion mismatch stress (~1 GPa) (Ref. 19) imposed on the interface) is ~250 MPa. Using a whisker strength of 8 GPa,[20] and assuming reasonable values of V^{po}/V^{fbl} (0.25) and the average of the l_{po}/l_{db} ratios (0.25), $\Delta J^{po}+\Delta J^{fbl}$ is found to be $2.5\Delta J^{fbl}$. This term then can be substituted for the ΔJ^{cb} term in Eq. (1*b*) to determine the contributions from both frictional bridging and pullout for SiC-whisker-reinforced aluminas (see next section). Note that l_{db} can be defined for the frictional debonded interface case using Eq. (8*b*) with $\sigma_y^l=\sigma_f^l$. Then, using the above values for τ_i, σ_f^l, and E^l, l_{db} is calculated to be approximately 6.5 μm. The ratio l_{po}/l_{db} (0.25) is consistent with the observed l_{po}/r ratio of ~4, i.e., $l_{po}=0.25(6.5\ \mu\text{m})\simeq 4(0.4\ \mu\text{m})$, respectively.

Similar evaluations of the relative contribution of pullout can be made for other composite systems using Eq. (12) and experimental observations. For instance, SiC-whisker-reinforced mullite and soda–lime-glass-matrix composites have thermal-expansion coefficients which are comparable with that of SiC. Thus, τ_i decreases; this coupled with the observed decrease in the l_{po}/r ratio indicates that the pullout contributions are markedly diminished in these two particular systems as compared with the alumina-based composite. Evaluation of these systems suggests that $\Delta J^{po}+\Delta J^{fb}\simeq 1.1\Delta J^{fb}$ for the mullite system and $\Delta J^{po}+\Delta J^{fb}\simeq\Delta J^{fb}$ for the soda–lime-glass-matrix composite based on the observation of the pullout parameters.

The frictional bridging versus pullout behaviors predicted are, of course, influenced markedly by the whisker strength and interfacial shear stress values. Although measurement of these two properties are, at best, difficult, we

can use experimental observations of interfacial debond lengths, pullout lengths, and the residual stresses imposed on the whiskers to make rational choices of these properties. This approach leads to the evaluation of the contribution of pullout as compared to frictional bridging. These evaluations of the relative contribution of pullout versus frictional bridging are quite useful because they provide a means to (1) describe the "toughening" effects derived from these two mechanisms and (2) indicate how a transition from the absence of pullout to extensive pullout (or vice versa) can significantly alter the fracture resistance of the composite.

The experimental fracture toughness results obtained in SiC-whisker-reinforced ceramics (Fig. 4) support the salient features of the models for frictional bridging and pullout as shown by a comparison of the experimental data with predicted curves. Here the predictions are based on analysis of the pullout of frictional bridging contributions (Eq. (15)) described in the previous paragraph. With this in mind, the toughening due to friction and pullout is calculated based on Eqs. (11*b*), (14*b*), and (15).

The results in Fig. 4 reveal several important features. First, both frictional bridging and pullout of the whisker reinforcement contribute to the fracture resistance as shown by comparing the predicted curves with the experimental results. This is particularly evident for the alumina composites, where frictional bridging based on Eq. (11*b*) accounts for a significant portion, but not all, of the toughening. However, it is known that pullout occurs in this system, and the inclusion of a pullout component with frictional bridging provides a good description of the observed behavior. This important contribution of pullout is further highlighted by the data for the alumina composite using the same SiC whiskers which had been oxidized prior to composite fabrication. The toughness of this composite falls on the frictional bridging curve (Fig. 4) consistent with the observed diminished pullout contribution.

Second, the fracture toughness due to bridging and pullout contributions does increase with volume/areal content of the reinforcing phase as predicted. Third, the toughening contributions increase as the ratio of Young's modulus of the composite to that of the whisker increases. This is best illustrated here by the increase in toughness due to crack bridging (Eqs. (11*a*) and (11*b*)) with increase in E^c at a given whisker content. For these examples, E^c values increase according to the rule of mixtures ($E^c = E^m(1-V_f) + E^w V_f$); thus, at a constant volume fraction of whiskers, E^c increases in the order from glass ($E^m = 80$ GPa) to mullite ($E^m = 210$ GPa) to alumina ($E^m = 400$ GPa) versus SiC ($E^w = 500$ GPa). This then contributes to the increase in frictional bridging contribution for alumina versus mullite versus glass at any given whisker content.

Earlier experimental observations[9] show that the frictional-bridging and the pullout-toughening contribution from the whiskers increases as r (the whisker radius) increases, as predicted by Eqs. (11*b*) and (14*b*). For example, the toughness of alumina composites containing 20 vol% SiC whiskers increases from ~6.5 to ~9 to ~12 MPa·m$^{1/2}$ when the mean diameter of the SiC whiskers increased from 0.3 to 0.75 to ~1.5 μm, respectively.

(3) Role of Material Properties and Characteristics

The model of the toughness contribution due to bridging by discontinuous, brittle reinforcing ligaments provides a very useful means of designing such composites and analyzing their response, as shown by the observations for whisker-reinforced ceramics and glasses (Fig. 4). In addi-

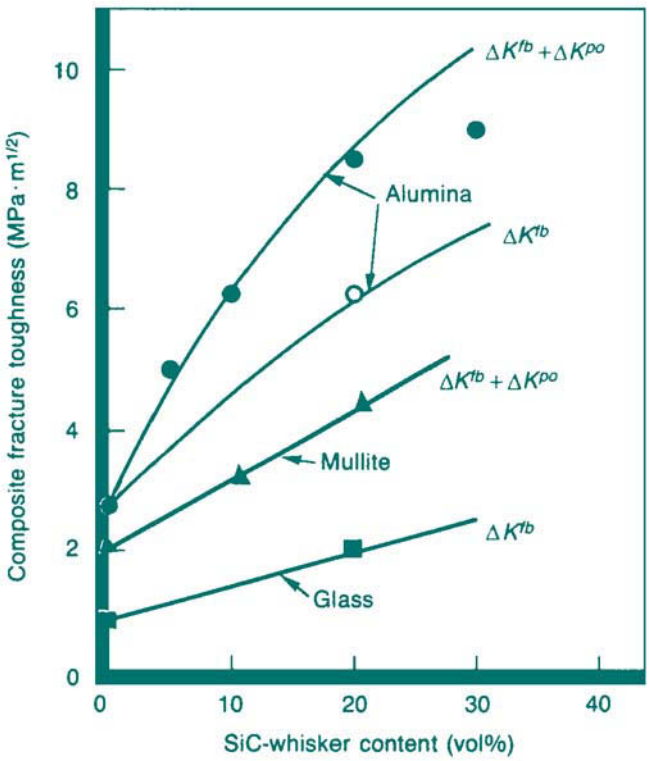

Fig. 4. Toughening contributions obtained by crack-bridging processes yield substantially increased fracture toughness. Curves represent the behavior predicted for frictional bridging, ΔK^{fb}, and the combined effects of frictional bridging plus pullout, ΔK^{po}, for alumina-, mullite-, and glass-matrix composites. Solid symbols indicate experimental data obtained with as-received 0.8-μm-diameter SiC whiskers; open circle is that for an alumina composite made with the same whiskers in a preoxidized condition.

tion, we can examine the effects of various characteristics on the toughness and consider what features may limit the toughness. The model also emphasizes that certain requirements are placed on the properties of the reinforcing phase and the matrix–reinforcement interfaces. A brief examination of some of the critical features is in order.

Note from Eqs. (11) and (14*b*) that toughening from the discontinuous reinforcement is greater when the matrix and reinforcing phase have comparable Young's moduli, when the reinforcing phase has very high fracture strength, and when the reinforcement content increases and its cross-sectional dimension (diameter) are large as discussed earlier. These features must be characterized (and not assumed) when developing composites. For example, examination of the whiskers would eliminate those that contain defects (e.g., large axial pores or large surface steps) which would be expected to reduce the whisker strength and pullout length. Other factors must be considered also. For example, the maximum diameter of the reinforcing phase which can be used will be limited by the thermal-expansion-coefficient (α) mismatch between the reinforcement and matrix. The larger thermal-expansion coefficient of the alumina matrix versus the SiC whiskers, which have a polyhedral cross section, coupled with the high Young's modulus of each, produces substantial axial (and hoop) tensile strains in the alumina, which increase with decreasing temperature[13b,21] (Fig. 5(A)). (Note that, at low temperatures, the mismatch stress does not change significantly because of the decrease in mismatch in the thermal-expression coefficients.) Earlier studies show that larger diameter SiC particles cause matrix cracking during postfabrication cooling and degrade the properties of such composites.[22] This is consistent with the increase in the stress intensity associated with these residual stresses and the greater propensity for microcracking with increase in size of the SiC whiskers. Thus, the maximum reinforcement diameter used may well depend on the elastic and thermal-expansion properties of the matrix versus those of the reinforcing phase.

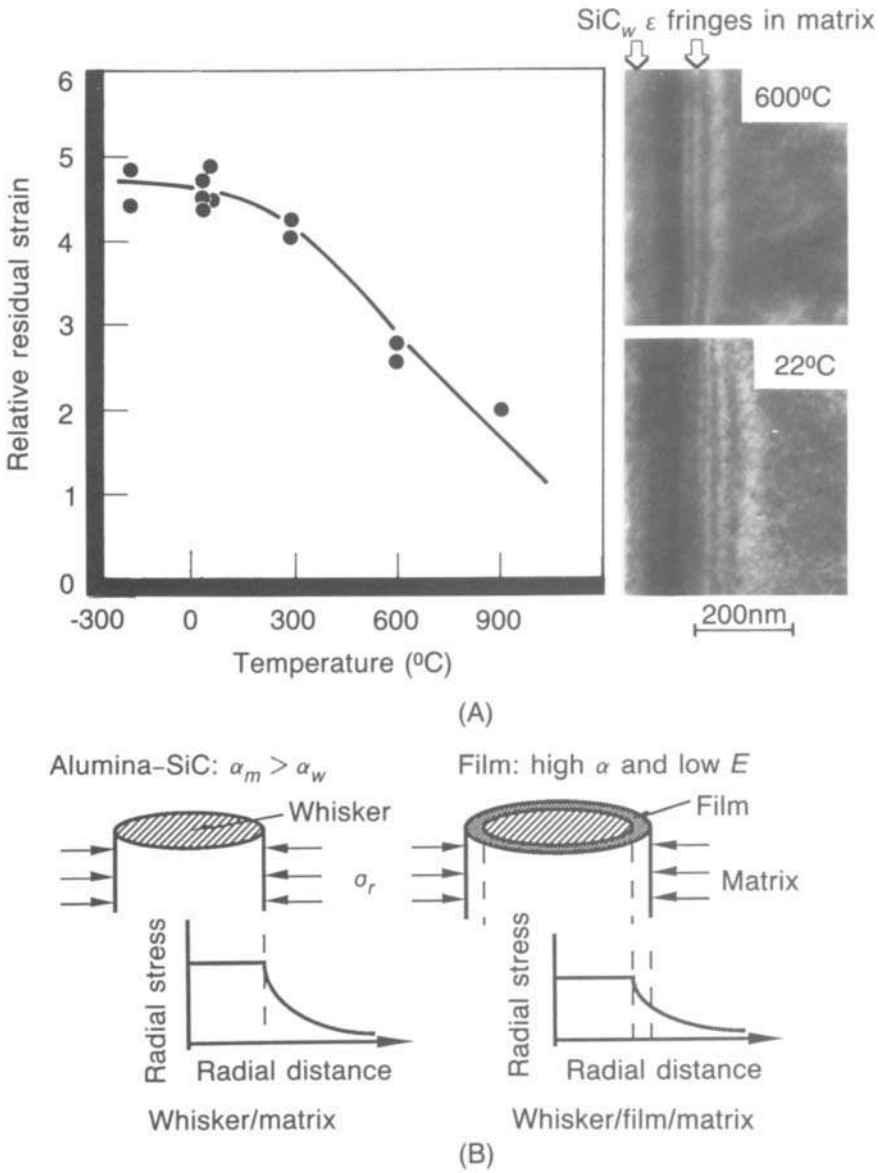

Fig. 5. Thermal-expansion mismatch radial compressive stress acting on the whisker–matrix interface restricts interface debonding and pullout. (A) Thermal-expansion-mismatch strain fringes observed in matrix increase in number during cooling, reflecting an increase in mismatch and stress. (B) Analytical studies show that such stresses can be reduced by incorporating proper interfacial film/layer.[23]

As noted earlier, debonding of the matrix–reinforcement interface during crack extension is one of the critical factors in such toughening processes. This occurs when the interfacial failure conditions are much less than those required to fracture the reinforcement. The formation of a debonded interface spreads the strain displacement imposed on the bridging reinforcing ligament over a longer gauge section, generating a larger crack-opening displacement per unit of stress supported by the ligament. As a result, the bridging traction/stress supported by the reinforcement increases more slowly with distance behind the crack tip, and a longer bridging zone is developed behind the crack tip. The resultant increase in crack-opening displacement with distance behind the crack tip (Eqs. (4) to (6) and (9)) significantly enhances the fracture resistance/toughness of the composite. The interfacial debonding process and subsequent straining and pullout of the reinforcement can be affected by residual stress and whisker surface morphology.

The mismatch in properties (as just noted) may be an important factor in

the choice of reinforcement–matrix combinations. However, this need not eliminate various combinations; i.e., the mismatch between alumina and the SiC whiskers is quite large, yet this is a very important example of toughening by discontinuous reinforcements. A key consideration, however, is that a very high radial compression (clamping) stress is imposed normal to the interface that may hinder interfacial debonding and pullout of debonded whiskers. If such expansion mismatch stresses could be reduced, pullout may be promoted. The analysis of Hsueh *et al.*[23] of these mismatch stresses reveals that interfacial films or coatings can be incorporated to diminish the radial compressive stress acting on the interface (Fig. 5(B)). For expansion mismatches similar to those in the SiC-whisker-reinforced alumina, an interfacial layer with a larger thermal-expansion coefficient and a low Young's modulus is desired. X-ray studies of SiC-whisker-reinforced alumina by Predecki *et al.*[19] confirm this effect using carbon coating on the whiskers to reduce mismatch stresses. Preliminary results indicate that the fracture toughness is indeed enhanced by the introduction of the carbon coating. This improved toughening effect can be attributed to the reduced clamping stress imposed on the whiskers; however, the coating may also reduce the interfacial debonding stress and thus increase the toughness.

In a similar manner, the pretreatment of the SiC whiskers noted earlier by the preoxidation of the whiskers can reduce the fracture resistance. On the other hand, heat treatments of the SiC whiskers under reducing conditions, which tend to reduce the surface oxygen content and enhance the surface carbon content, yield whiskers which produce greater fracture toughness.[9] Finally, another aspect that is deemed important is that the interface be relatively straight and smooth. Whiskers that have very corrugated surfaces with deep reentrant corners could result in a mechanically interlocked (zigzagged) interface. Such interlocking interfaces are expected to be much more resistant to debonding. For example, studies of gold–glass interfaces show that the Mode I fracture energy for interfacial cracks is reduced by an order of magnitude for a flat interface versus a mechanically interlocked interface.[24] In addition, such surface features could (1) act as stress concentrations and reduce the whisker strength and/or (2) limit pullout.

(4) Crack Bridging by Other Brittle Reinforcements

Discontinous brittle reinforcements of various geometries are found to impart toughness to ceramics. These reinforcements include second-phase platelets[25–27] and elongated,[27–31] platelike,[32] and/or large[14,33–36] matrix grains. Observations of the wake of the crack-tip region in these systems indicate that these reinforcements also bridge the crack. In this section we review some of the toughening effects observed in ceramics reinforced by such features. The influence of the matrix microstructure (e.g., both elongated and larger grains) is of particular interest because this also provides a means of modifying the matrix microstructure to obtain additional toughening as we shall show later.

(A) Crack Bridging by Noncubic Matrix Grains: Size Effects: In noncubic ceramics, bridging ligaments are often formed by matrix grains that are left intact behind the crack tip and thus provide for increased toughness.[34–36] As noted in alumina ceramics, the toughness increases with increasing grain size[33–36] up to a critical grain size above which spontaneous matrix microcracking and microcrack linkage degrades the toughness.[33] This toughening behavior is analogous to that for the whisker reinforcement described earlier and is analyzed here using a similar approach; i.e., the additional energy consumed by the bridging zone is defined as the product of the bridging stress and crack-opening displacement. However, the bridging stress supported by ligaments, formed possibly by microcracking along grain boundaries, can be shown to be the product of the frictional shear stress required to pull out each bridging grain, τ_{gb}, times the fraction of bridging grains, A^{gb}, as discussed in a separate paper.[35] Other types of matrix-bridging processes and their contribution to the fracture toughness have been discussed recently.[36] As we formulated earlier, the grain-bridging zone length is dictated by equating the crack-opening displacement at the end of the zone, u^*, to that required to completely pull out the bridging grains. Assuming that one-half of the grains must be pulled out to disrupt a ligament, u^* is equal to one-half the grain size, d, and the incremental increase in strain energy release rate due to grain bridging, ΔJ^{gb}, is

$$\Delta J^{gb} = A^{gb}\tau_{gb}d/2 \qquad (16a)$$

The J^m term in Eq. (1*b*) then becomes

$$J^m = J^o + A^{gb}\tau_{gb}d/2 \qquad (16b)$$

Substituting Eq. (16*b*) for the J^m terms in Eq. (1*a*) allows us to determine the fracture toughness effects due to grain size in noncubic composites. The model is consistent with experimental observations as noted in Fig. 6, where the experimental fracture toughness of unreinforced alumina (V^w=0%) is found

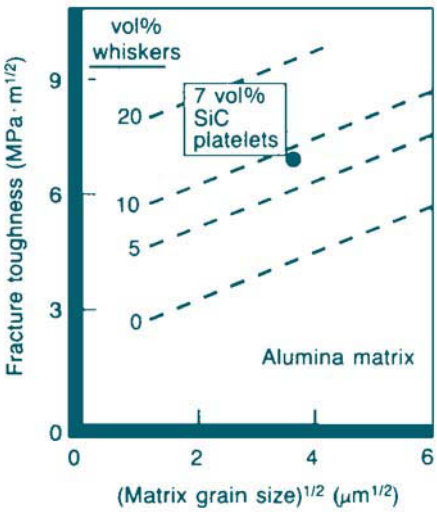

Fig. 6. Fracture toughness of alumina ceramics is enhanced by increase in the matrix grain size. Similar toughening effects due to grain size/grain bridging are observed in SiC-whisker-reinforced alumina. Substitution of SiC platelets results in toughening contribution which is comparable to that obtained with whiskers.

to increase with increase in the square root of the matrix grain size.

(B) Platelet and Rodlike Reinforcements: Matrix Grains and Second Phases: Other reinforcing-phase geometries, aside from whiskers, can result in crack-bridging phenomena and enhanced toughening effects. Earlier work on alumina ceramics has produced microstructures that contained large (100 to 200 μm across by ~10 μm thick) platelike alumina grains in a medium-sized (~5 μm), equiaxed, grained matrix.[32] These materials have excellent thermal-shock resistance; in fact, their thermal-shock resistance is much greater than that of any of the varieties of ceramics tested, including zirconias, various other oxides, silicon nitrides, and aluminas with equiaxed grains. Further examination shows that samples containing ~25 vol% of these large single-crystal alumina plates have fracture-toughness values of ~7 MPa·m$^{1/2}$. The large face dimensions of the platelike grains do reduce the strength of the material; thus, we must modify the plate size to optimize strength and toughness. On the other hand, aluminas with only the ~5-μm-equiaxed grains have toughness values of only 4 to 4.5 MPa·m$^{1/2}$. Microscopy observation of the aluminas containing the platelike grains reveal that cracks deflected along the interface between the matrix and the large platelike grains. This produces plates that bridge the main crack and contribute to the high toughness in much the same manner as do SiC whiskers.

We can perceive that the logical extension is to consider whether or not crack bridging by second-phase platelets contributes to fracture toughness. Work by Hori *et al.*[25] reveals that composites composed of an equiaxed polycrystalline matrix of titania with dispersed alumina platelets exhibit an increase in fracture resistance. Specifically, this work shows that, under conditions where the platelet dimensions remain fairly constant, the toughness increases with increasing platelet content leading to nearly a threefold increase with 30 vol% of alumina platelets. In our own studies, alumina has also been found to be toughened by the addition of SiC platelets.[26] An example is seen in Fig. 6, which reveals that, for a comparable matrix grain size, the particular SiC platelets[†] used yield an increase in fracture toughness that is similar to that achieved with SiC whiskers. Microscopy observations of these composites show that crack bridging by the reinforcement is again occurring.

Perhaps one of the most intriguing areas is the reinforcement of silicon nitride[28-30] and SiAlON[31] ceramics by the in situ growth of elongated or whisker-like grains. Numerous experimental results reveal that this is also a potent toughening approach resulting in toughness values in excess of 10 MPa·m$^{1/2}$ in the silicon nitride ceramics. Such materials have been labeled as self-reinforced, and, from the crack observations of Li and Yamanis,[29] crack bridging by these elongated grains contributes to the improved toughness. Sufficient additional experimental results exist for us to begin to test how well the current crack-bridging models describe the toughening effects of such elongated grains.

The results of Tajima *et al.*[37] show that the toughening contribution from crack bridging increases with increase in volume content of the elongated grains. More recent observations also reveal that the bridging contribution increases with increase in the cross-sectional dimension of the elongated grains (Fig. 7). In fact, these authors have shown that K^c is proportional to the square root of the diameter of the elongated grains,[38] which is in excel-

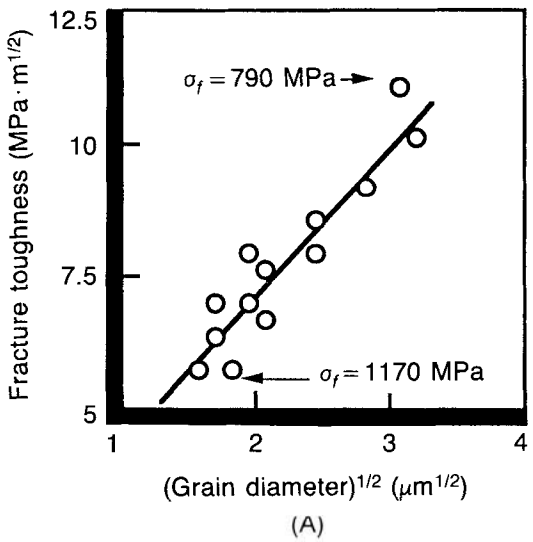

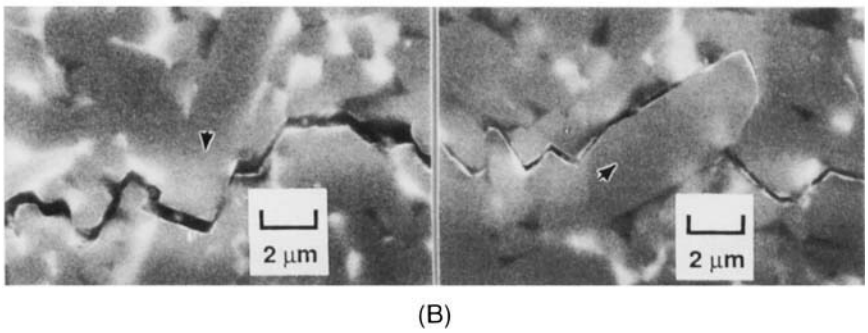

Fig. 7. Fracture toughness of self-reinforced silicon nitride can be increased in the presence of elongated grains. (A) Data from H. Okamoto and T. Kawashima[38] illustrate the increase in toughness with increase in diameter of the elongated grains. (B) Toughening is associated with crack bridging and pullout of the elongated matrix grains (H.T. Lin[39]).

[†]Superfine grade SiC platelets, C-Axis Technology, Clark Summit, PA.

lent agreement with the behavior predicted for crack-bridging processes by Eqs. (8), (11*a*), (11*b*), and (14*b*). These diverse sources of observations support crack bridging by the elongated grains as an important toughening process in these silicon nitride ceramics (Fig. 7). As shown in Fig. 7, these self-reinforced silicon nitrides exhibit excellent fracture strengths as well.

(5) Coupled-Toughening Responses

An area of remarkable potential is the coupling of two or more toughening mechanisms within the same composite. The possibility exists to design ceramic composites with discontinuous reinforcing phases to achieve fracture toughness values in excess of 10 MPa·m$^{1/2}$, i.e., approaching 20 MPa·m$^{1/2}$. From the foregoing discussions, it is apparent that second-phase reinforcements, such as whiskers and platelets, combined with matrix microstructural tailoring may offer such potential. In addition, reinforcement by a discontinuous second phase could be combined with transformation toughening. Each of these is briefly considered in the following sections.

(A) Whisker Reinforcement Coupled with Matrix Grain Bridging: As discussed earlier, the fracture resistance of ceramics, especially noncubic ceramics, increases with increase in the grain size as a result of grain bridging in the wake of the crack tip. Thus the overall fracture toughness of the composite can also be influenced by the intrinsic matrix toughness, the microstructural component of the matrix toughness (especially in the case of noncubic matrices), and the whisker-reinforcement contribution.[35] For a simple additive combination of these toughening processes in Eq. (1*b*), the overall composite toughness is

$$K_{IC}^{c}=[E^{c}(J^{o}+\Delta J^{gb}+\Delta J^{wr})]^{1/2} \qquad (17a)$$

where ΔJ^{gb} is the energy consumed by matrix grain bridging (Eq. (16*a*)), ΔJ^{wr} includes whisker bridging and pullout contributions, and J^{o} is the energy consumption by lattice bond rupture. Substitution of Eq. (16*b*) into Eq. (17*a*) describes the combined toughness:

$$K_{IC}^{c}=[(J^{o}+V_{gb}\tau_{gb}d/2+\Delta J^{wr})E^{c}]^{1/2} \qquad (17b)$$

This coupled-toughening behavior is observed in SiC-whisker-reinforced aluminas (Fig. 6). The matrix microstructure can be readily modified using multiple toughening mechanisms to further enhance the fracture toughness of a com-posite by increasing the matrix grain size. Thus we must develop/optimize those parameters controlling the whis-ker reinforcement and matrix micro-structural toughening contribution to take full advantage of these materials.

Because of the crack-bridging toughening contribution from the elongated matrix grains in silicon nitrides, we might expect that reinforcement with SiC whiskers could be combined with that from the elongated matrix grains to further enhance the toughness. This appears to be the case. Let us reconsider the data by Shalek *et al.*,[40] which indicate that a hot-pressed, fine-grained silicon nitride can be toughened by the addition of SiC whiskers (Fig. 8) in a manner predicted by Eqs. (7), (11*b*), and/or (14*b*). In these cases, lower processing temperatures appear to generate a fine-grained matrix, whereas high temperatures produce elongated matrix grains and higher toughness. Combined with this is the fact that, with an increase in whisker content, it becomes more difficult to generate the elongated matrix grains (whiskers can be effective grain-growth inhibitors). Thus, although we can combine toughening due to the elongated matrix grains and the whiskers, greater variability in the fracture toughness may be achieved as the whisker content is increased in these self-reinforced silicon nitrides (Fig. 8). Recent studies of Chu and Singh[41] further illustrate the important contribution of the presence of the elongated matrix grains in promoting the toughness of whisker-reinforced silicon nitride composites.

(B) Whisker Reinforcement Plus Transformation Toughening: The fracture toughness, K^{c}, of tetragonal zirconia-toughened composites can be

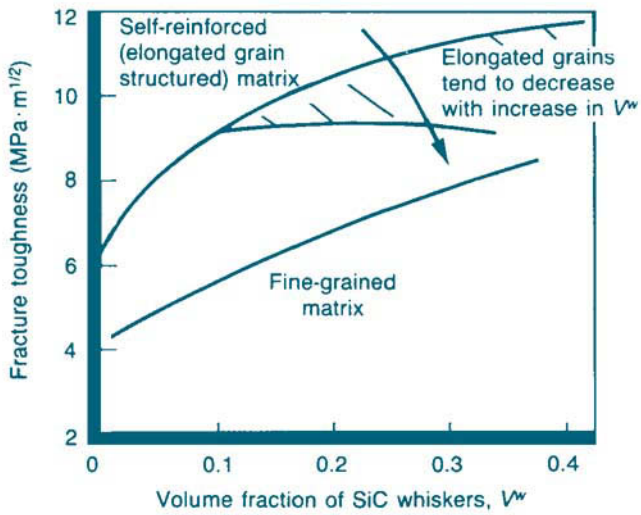

Fig. 8. Fracture toughness of silicon nitride ceramics reinforced with SiC whiskers is dependent on the silicon nitride matrix microstructure. A fine-grained matrix exhibits lower toughness than when elongated matrix grains are formed. Presence of SiC whiskers often inhibits the growth of elongated matrix grains.

described by

$$K^c = K^m + \Delta K^T \quad (18a)$$

where ΔK^T is given by

$$\Delta K^T = A(\epsilon^T) E^c V^T r_T^{1/2} \quad (18b)$$

and defines the contribution associated with the stress-induced transformation of tetragonal-zirconia particles or grains. In Eq. (18*b*), A is a constant related to the stress state, ϵ^T is the transformation strain, and V^T is the volume fraction of zirconia that actually transforms. As shown here, ΔK^T is proportional to the transformation zone size, $(r_T)^{1/2}$.[11a] However, using a small-scale yielding criteria, we can show that the magnitude of r_T is dependent upon the ratio of the matrix toughness to the critical transformation stress, σ_c^T, required to transform the tetragonal zirconia ($\propto K^m/\sigma_c^T$).[11c,42] This simply means that, the greater the resistance of the matrix to fracture, the greater the distance away from the crack where the stress is sufficient to transform the tetragonal zirconia. Thus, in a composite matrix containing tetragonal zirconia, increasing the matrix toughness raises the toughness of the composite in two steps: first, by simply enhancing the matrix toughness (Eq. (18*a*)), and, second, by the transformation-toughening contribution (Eq. (18*b*)) where $r_T \propto K^m$.

If we use the preceding approaches to toughen the matrix in combination with transformation toughening, a synergistic toughening effect should be possible. Earlier studies[43] show that combining transformation toughening with reinforcement by a discontinuous second phase can result in a toughening response that is larger than simply additive. To illustrate this, mullite composites containing reinforcing SiC whiskers with and without dispersed zirconia particles were evaluated. All samples were tested at 800°C because samples could be treated to produce either monoclinic-zirconia or tetragonal-zirconia particles. The tetragonal-zirconia particles in this case spontaneously transformed from the tetragonal to the monoclinic phase on cooling to ~750°C, the M_s temperature. On heating, all monoclinic particles converted to the tetragonal phase at ~1050°C. Thus, at 800°C, which is only slightly above the M_s temperature, it is quite easy to transform tetragonal zirconia; i.e., σ_c^T is small, and strong transformation-toughening effects occur when these particular zirconia particles are in the tetragonal phase.[43] This is illustrated for results obtained at 800°C in Fig. 9, which shows that mullite reinforced with 20 vol% SiC whiskers is toughened by a factor of ~2 times that of the unreinforced mullite. At this same test temperature, the addition of monoclinic-zirconia particles to the whisker-reinforced mullite produces a composite with a toughness that is approximately 3.5-fold that of mullite.[43] The combined effects of whisker reinforcement and monoclinic zirconia here are simply additive (Fig. 9). However, when the same volume percent of zirconia particles are in the tetragonal phase, the combined toughening results in a much greater toughening effect (e.g., fivefold to 5.5-fold increase in toughness) (Fig. 9). Similar strong toughening effects have been described by Claussen *et al.*[14] These findings confirm the strong coupled-toughening behavior predicted by Eq. (18) and suggest continuing efforts to improve the transformation-toughening response by the addition of reinforcing phases.

Based on earlier studies of transformation-toughened ceramics,[42] the toughness of these types of composites are a function of the test temperature when transformation toughening occurs. The extent of the transformation-toughening contribution is also determined by the alloy content, volume content, and size of the transformable zirconia particles. The latter factors also indicate that processing of such composites requires careful selection of compositions and advanced processing technology to achieve the desired microstructures. However, a multiple toughening mechanism approach provides a means of obtaining substantial additional increases in fracture resistance.

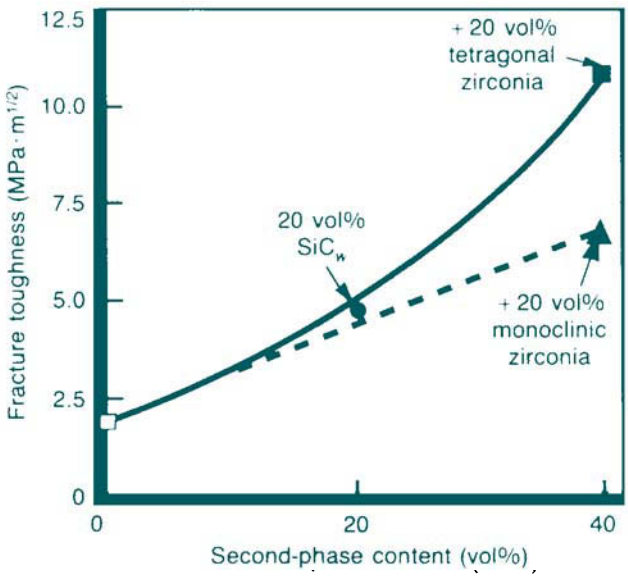

Fig. 9. Greater fracture resistance can be achieved via coupled-toughening effects, combining whisker reinforcement with zirconia toughening in a ceramics matrix. Whisker reinforcement and transformation toughening associated with the dispersed tetragonal-zirconia particles were combined to raise the toughness of mullite by more than fivefold.

III. Concluding Remarks

Over the years considerable effort has been expended by the ceramics community to develop processing approaches leading to dense, very fine equiaxed grained, single-phase (where possible), polycrystalline ceramics with minimum defect sizes and minimum defect-size distributions. The goal has been the development of ceramics with improved fracture strengths; in fact, some still wish to produce ceramics with strength in excess of 1 GPa in this manner. As Lange[2] observes, the processing must control the source of all potential defects. In fact, it is not clear that ultrahigh strengths are needed for a great majority of the current and future applications of ceramics. We are more concerned with the mechanical reliability of ceramics. High initial strength is not a solution if the material is readily degraded as a result of service conditions. We must also look for approaches to overcome the low fracture toughness of ceramics if we are to avoid damage and attendant loss of strength.

As discussed here, we now need to readdress microstructural design of structural ceramics (e.g., materials with high fracture toughness and useful strength) to take advantage of toughening by crack-bridging processes. We see from earlier discussions that the incorporation of discontinuous, elastic reinforcing phases (e.g., whiskers, platelets) promotes crack-bridging processes and achieves significant toughening. However, this approach also requires attention to those parameters (e.g., interfacial structure and properties, reinforcement strength, morphology, size, and mismatch between matrix and reinforcement) that control the toughening contribution. In addition to examples already cited, we note, for example, that not all whiskers are the same in terms of defects and strength, which limits the toughening contribution. Similarly, smooth whisker surfaces are beneficial in the interfacial debonding required for the crack-bridging contribution to toughening.

However, the design of toughened ceramics must, where possible, seek to optimize the matrix microstructure when grain shape and size can be used to obtain greater fracture resistance by crack bridging. Matrix microstructural design is, perhaps, best illustrated by the self-reinforced silicon nitrides where large *elongated* grains can contribute to both high fracture strength and high fracture toughness. Another classic example is the aluminas with larger grains (either "equiaxed" or platelike) which have high toughness. However, we are reminded that the incorporation of large matrix grains, second-phase platelets, and platelike matrix grain structures to toughen the ceramics can result in lower strengths. Toughening by large grains and platelets is based on the ease of interfacial debonding. The large two-dimensional platelet or grain surfaces could also readily act as flaws. This simply means that we must be prepared to make some trade-offs in platelet dimensions in designing for strength and/or toughness. In an instance where high strength was not needed but high damage resistance due to thermal shock was needed, aluminas toughened by the incorporation of platelet alumina grains readily met the service requirements. The trade-offs in grain size in noncubic ceramics (e.g., aluminas) offer an option to *optimize* the *overall* or *specific* mechanical properties rather than limiting these properties.

Combining various toughening processes, e.g., matrix with reinforcement bridging or reinforcement bridging with transformation toughening, offers the opportunity to develop very tough (10 to 20 $MPa \cdot m^{1/2}$) ceramic composites. We will be remiss if these combined toughening processes are not used. From even these limited considerations, we can see that there is tremendous potential for enhancing the mechanical performance of ceramics by such microstructural design approaches. Again, attention to a variety of microstructural and phase properties will be required, but herein lies the opportunity to develop toughened ceramics. With these opportunities come challenges to the processing and materials design communities.

Acknowledgments: The technical contributions of T.N. Tiegs, C.H. Hsueh, K.B. Alexander, P. Angelini, H.T. Lin, M.K. Ferber, S.B. Waters, and W.H. Warwick of Oak Ridge National Laboratory (ORNL) and E.R. Fuller, Jr., of National Institute of Standards and Technology (NIST) are gratefully acknowledged. The author also recognizes the efforts of L.M. Evans, who prepared the manuscript, C.T. Liu and M.K. Ferber of ORNL who reviewed it, and the insightful comments of E.R. Fuller, NIST.

References

[1](a) A. Kelly and N.H. Macmillan, *Strong Solids*; pp. 375–77. Claredon Press, Oxford, U.K., 1986. (b) W.S. Pellini, *Principles of Structural Integrity Technology*; pp. 63–85. U.S. Government Printing Office, Washington, DC, 1976.

[2]F.F. Lange, "Processing Science and Technology for Increased Reliability," *J. Am. Ceram. Soc.*, **72** [1] 3–15 (1989).

[3]A.A. Griffith, "The Phenomena of Rupture and Flow in Solids," *Philos. Trans. R. Soc. London*, **A221**, 163 (1920).

[4]J.F. Rhodes, "Alumina and Alumina Composites"; presented at Gorham International Conference, Monterey, CA, April 1985.

[5]K.C. Liu, Oak Ridge National Laboratory; unpublished results.

[6](a) F.F. Lange, "The Interaction of a Crack Front with a Second-Phase Dispersion," *Philos. Mag.*, **22** [179] 983–92 (1970). (b) A.G. Evans, "The Strength of Brittle Materials Containing Second-Phase Dispersions," *Philos. Mag.*, **22**, 1327–44 (1972). (c) F.F. Lange, "Fracture Energy and Strength Behavior of a Sodium Borosilicate Glass–Al_2O_3 Composite System," *J. Am. Ceram. Soc.*, **54** [12] 614–20 (1971).

[7](a) K.T. Faber and A.G. Evans, "Crack Deflection Processes–I, Theory," *Acta Metall.*, **31** [4] 565–76 (1983). (b) K.T. Faber and A.G. Evans, "Crack Deflection Processes–II, Experiment," *Acta Metall.*, **31** [4] 577–84 (1983). (c) G.C. Wei and P.F. Becher, "Improvements in Mechanical Properties in SiC by the Addition of TiC Particles," *J. Am. Ceram. Soc.*, **67** [8] 571–74 (1984).

[8](a) A. Kelly, *Strong Solids*; pp. 157–226. Claredon Press, Oxford, U.K., 1973. (b) K.M. Prewo and J.J. Brennan, "High-Strength Silicon Carbide-Fibre-Reinforced Glass-Matrix Composites," *J. Mater. Sci.*, **15** [2] 463–68 (1980). (c) D.B. Marshall, B.N. Cox, and A.G. Evans, "Mechanics of Matrix Cracking in Brittle-Matrix Composites," *Acta Metall.*, **33** [11] 2013–21 (1985). (d) A.G. Evans and R.M. McMeeking, "Toughening of Ceramics by Strong Reinforcements," *Acta Metall.*, **34** [12] 2435–41 (1986). (e) M.R. Piggott, *Load Bearing Fiber Composites*; pp. 100–40. Pergamon Press, Elmsford, NY, 1980. (f) R.W. Rice, "Mechanisms of Toughening in Ceramic Matrix Composites," *Ceram. Eng. Sci. Proc.*, **2** [7–8] 661–701 (1981). (g) J. Homeny, W.L. Vaugh, and M.K. Ferber, "Processing and Mechanical Properties of SiC-Whisker-Al_2O_3-Matrix Composites," *Am. Ceram. Soc. Bull.*, **65** [2] 333–38 (1986). (h) G.H. Campbell, M. Rühle, B.J. Dalgleish, and A.G. Evans, "Whisker Toughening: A Comparison between Al_2O_3 and Si_3N_4 Toughened with SiC," *J. Am. Ceram. Soc.*, **73** [3] 521–30 (1990). (i) K.P. Gadkaree and K. Chyung, "Silicon Carbide-Whisker-Reinforced Glass and Class-Ceramics," *J. Am. Ceram. Soc.*, **73** [3] 370–76 (1990). (j) S.V. Nair, "Crack-Wake Debonding and Toughness in Fiber- or Whisker-Reinforced Brittle-Matrix Composites," *J. Am. Ceram. Soc.*, **73** [10] 2839–47 (1990).

[9]P.F. Becher, C.H. Hsueh, P. Angelini, and T.N. Tiegs, "Toughening Behavior in Whisker-Reinforced Ceramic Matrix Composites," *J. Am. Ceram. Soc.*, **71** [12] 1050–61 (1988).

[10](a) R.W. Rice, "Microstructure Dependence of Mechanical Behavior of Ceramics"; pp. 199–381 in *Treatise on Materials Science and Technology*, Vol. 11. Edited by R.K. MacCrone. Academic Press, New York, 1977. (b) N. Claussen, J. Steeb, and R.F. Pabst, "Effect of Induced Microcracking on the Fracture Toughness of Ceramics," *Am. Ceram. Soc. Bull.*, **56** [6] 559–62 (1977). (c) D.J. Magley, R.A. Winholtz, and K.T. Faber, "Residual Stresses in a Two-Phase Microcracking Ceramic," *J. Am. Ceram. Soc.*, **73** [6] 1641–44 (1990). (d) M. Rühle, N. Claussen, and A.H. Heuer, "Transformation and Microcrack Toughening as Complementary Processes in ZrO_2-Toughened Al_2O_3," *J. Am. Ceram. Soc.*, **69** [3] 195–97 (1986).

[11](a) R.M. McMeeking and A.G. Evans, "Mechanics of Transformation-Toughening in Brittle Materials," *J. Am. Ceram. Soc.*, **65** [5] 242–46 (1982). (b) A.G. Evans, "High-Toughness Ceramics," *Mater. Sci. Eng. A*, **105/106**, 65–75 (1988). (c) A.G. Evans and R.M. Cannon, "Toughening of Brittle Solids by Martensitic Transformations," *Acta Metall.*, **34** [5] 761–800 (1986). (d) D. Green, R.H.J. Hannink, and M.V. Swain, *Transformation Toughening of Ceramics*. CRC Press, Boca Raton, FL, 1989.

[12](a) V.V. Krstic, P.S. Nicholson, and R.G. Hoagland, "Toughening of Glasses by Metallic Particles," *J. Am. Ceram. Soc.*, **64** [9] 499–504 (1981). (b) J.L. Chermant and F. Osterstock, "Fracture Toughness and Fracture of WC–Co Composites," *J. Mater. Sci.*, **11**, 1939–51 (1976). (c) L.S. Sigl, P.A. Mataga, B.J. Dalgleish, R.M. McMeeking, and A.G. Evans, "On the Toughness of Brittle Materials Reinforced with a Ductile Phase," *Acta Metall.*, **36** [4] 945–53 (1988). (d) B.D. Flinn, M. Rühle, and A.G. Evans, "Toughening of Composites of Al_2O_3 Reinforced with Al," *Acta Metall.*, **37** [11] 3001–3006 (1989). (e) J.P. Pickens and J. Gurland, "The Fracture Toughness of WC–Co Alloys Measured on Single-Edge Notched-Beam Specimens Precracked by Electron-Discharge Machining," *Mater. Sci. Eng.*, **33**, 135–42 (1978).

[13](a) P.F. Becher and G.C. Wei, "Toughening Behavior in SiC-Whisker-Reinforced Alumina," *J. Am. Ceram. Soc.*, **67** [12] C-267–C-269 (1984). (b) P.F. Becher, "Recent Advances in Whisker-Reinforced Ceramics"; pp. 179–95 in *Annual Review of Materials Science*, Vol. 20. Edited by R.A. Huggins. Annual Review, Palo Alto, CA, 1990.

[14]N. Claussen and G. Petzow, "Whisker-Reinforced Zirconia-Toughened Ceramics"; pp. 649–62 in *Tailoring of Multiphase and Composite Ceramics*, Vol. 20, Materials Science Research. Edited by R.E. Tressler, G.L. Messing, C.G. Pantano, and R.E. Newnham. Plenum, New York, 1986.

[15]P.F. Becher, T.N. Tiegs, and P. Angelini, "Whisker-Toughened Ceramic Composites"; pp. 311–27 in *Fiber Reinforced Ceramics*. Edited by K.S. Mazdiyasni. Noyes, Park Ridge, NJ, 1990.

[16]R. Warren and V.K. Sarin, "Fracture of Whisker-Reinforced Ceramics"; in *Applications of Fracture Mechanics to Composite Materials*. Edited by K. Friedrich. Elsevier, Amsterdam, Netherlands, in press.

[17]J.R. Rice; pp. 191–205 in *Fracture*, Vol. II. Edited by H. Liebowitz. Academic Press, New York, 1986.

[18]B. Budiansky, J.W. Hutchinson, and A.G. Evans, "Matrix Fracture in Fiber-Reinforced Ceramics," *J. Mech. Phys. Solids*, **34** [2] 167–89 (1986).

[19]P. Predecki, A. Abuhasan, and C.S. Barrett, "Residual Stress Determination in Al_2O_3/SiC (Whisker) Composites by X-ray Diffraction"; pp. 231–43 in *Advances in X-ray Analysis*, Vol. 13. Edited by C.S. Barrett, J.V. Gilfrich, R. Jenkins, J.C. Russ, Jr., W. Richardson, Jr., and P.K. Predecki. Plenum, New York, 1988.

[20]J.J. Petrovic, J.V. Milewski, D.L. Rohr, and R.D. Gac, "Tensile Mechanical Properties of SiC Whiskers," *J. Mater. Sci.*, **20**, 1167–77 (1985).

[21]P. Angelini, W. Mader, and P.F. Becher, "Strain and Fracture in Whisker-Reinforced Ceramics"; pp. 241–57 in MRS Proceedings, *Advanced Structural Ceramics*, Vol. 78. Edited by P.F. Becher, M.V. Swain, and S. Sōmiya. Materials Research Society, Pittsburgh, PA, 1987.

[22]T.N. Tiegs, "Tailoring Properties of SiC Whisker–Oxide Matrix Composites"; pp. 937–49 in *Ceramic Materials and Components for Engines*.

Edited by V.J. Tennery. American Ceramic Society, Westerville, OH, 1989.

[23]C.H. Hsueh, P.F. Becher, and P. Angelini, "Effects of Interfacial Films on Thermal Stress in Whisker-Reinforced Ceramics," *J. Am. Ceram. Soc.*, **71** [11] 929–33 (1988).

[24]P.F. Becher and W.L. Newell, "Adherence–Fracture Energy of a Glass-Bonded Thick-Film Conductor: Effect of Firing Conditions," *J. Mater. Sci.*, **12**, 90–96 (1977).

[25]S. Hori, H. Kaji, M. Yoshimura, and S. Sōmiya, "Deflection-Toughened Corundum–Rutile Composites"; pp. 283–88 in MRS Proceedings, *Advanced Structural Ceramics*, Vol. 78. Edited by P.F. Becher, M.V. Swain, and S. Sōmiya. Materials Research Society, Pittsburgh, PA, 1987.

[26]K.B. Alexander, P.F. Becher, and S.B. Waters, "Characterization of Silicon Carbide Platelet-Reinforced Alumina"; pp. 106–107 in *Proceedings of Twelfth International Congress for Electron Microscopy*. San Francisco Press, San Francisco, CA, 1990.

[27]F.J. Cambier, "Processing and Properties of SiC-Platelet Silicon Nitride Ceramics"; to be published in *Proceedings of the International Workshop for Fine Ceramics: New Processing and Properties of Fine Ceramics* (Nagoya, Japan, March 15–16, 1990).

[28]F.F. Lange, "Fracture Toughness of Si_3N_4 as a Function of the Initial α-Phase Content," *J. Am. Ceram. Soc.*, **62** [7–8] 428–30 (1979).

[29]C.W. Li and J. Yamanis, "Super-Tough Silicon Nitride with *R*-Curve Behavior," *Ceram. Eng. Sci. Proc.*, **10** [7–8] 632–45 (1989).

[30]G. Himsolt, H. Knoch, H. Huebner, and F.W. Kleinlein, "Mechanical Properties of Hot-Pressed Silicon Nitride with Different Grain Structures," *J. Am. Ceram. Soc.*, **62** [1] 29–32 (1979).

[31]M.H. Lewis, "Microstructural Engineering of Ceramics for High-Temperature Application"; pp. 713–30 in *Fracture Mechanics of Ceramics*, Edited by R.C. Bradt, A.G. Evans, D.P.H. Hasselman, and F.F. Lange. Plenum, New York, 1986.

[32]T.N. Tiegs and P.F. Becher, "Particulate- and Whisker-Toughened Alumina Composites"; pp. 479–85 in *Proceedings of 22nd Automotive Technology Development Contractors' Coordination Meeting*, Vol. P-155. Society of Automotive Engineers, Warrendale, PA, 1985.

[33](a) R.W. Rice, S.W. Freiman, and P.F. Becher, "Grain-Size Dependence of Fracture Energy in Ceramics: I, Experiment," *J. Am. Ceram. Soc.*, **64** [6] 345–50 (1981). (b) B. Mussler, M.V. Swain, and N. Claussen, "Dependence of Fracture Toughness of Alumina on Grain Size and Test Technique," *J. Am. Ceram. Soc.*, **65** [11] 566–72 (1982). (c) R.F. Cook, "Segregation Effects in the Fracture of Brittle Materials: $CaAl_2O_3$," *Acta Metall.*, **38** [6] 1083–100 (1990). (d) R. Steinbrech, R. Khehans, and W. Schaarwachter, "Increase of Crack Resistance During Slow Crack Growth in Al_2O_3 Bend Specimens," *J. Mater. Sci.*, **18** 265–70 (1983).

[34](a) P.L. Swanson, C.J. Fairbanks, B.R. Lawn, and Y.W. Mai, "Crack-Interface Grain Bridging as a Fracture Resistance Mechanism in Ceramics: I, Experimental Study of Alumina," *J. Am. Ceram. Soc.*, **70** [4] 279–89 (1987). (b) Y.W. Mai and B.R. Lawn, "Crack-Interface Grain Bridging as a Fracture Resistance Mechanism in Ceramics: II, Theoretical Fracture Mechanics Model," *J. Am. Ceram. Soc.*, **70** [4] 289–94 (1987).

[35]P.F. Becher, E.R. Fuller, Jr., and P. Angelini, "Matrix Grain Bridging in Whisker-Reinforced Ceramics," *J. Am. Ceram. Soc.*, in review.

[36](a) S.T. Bennison and B.R. Lawn, "Role of Interfacial Grain-Bridging Friction in the Crack-Resistance and Strength Properties of Nontransforming Ceramics," *Acta Metall.*, **37** [10] 2659–71 (1989). (b) G. Vekinis, M.F. Ashby, and P.W.R. Beaumont, "*R*-Curve Behavior of Al_2O_3 Ceramics," *Acta Metall.*, **38** [6] 1151–62 (1990).

[37]Y. Tajima, K. Urashima, M. Watanabe, and Y. Matsuo, "Fracture Toughness and Microstructure Evaluation of Silicon Nitride Ceramics"; pp. 1034–41 in Ceramic Transactions, Vol. 1, *Ceramic Powder Science-IIB*. Edited by G.L. Messing, E.R. Fuller, Jr., and H. Hausner. American Ceramic Society, Westerville, OH, 1988.

[38]H. Okamoto and T. Kawashima; unpublished results.

[39]H.T. Lin, Oak Ridge Associated Universities–Oak Ridge National Laboratory; unpublished results.

[40]P.D. Shalek, J.J. Petrovic, G.F. Hurley, and F.D. Gac, "Hot-Pressed SiC Whisker/Si_3N_4 Matrix Composites," *Am. Ceram. Soc. Bull.*, **65** [2] 351–56 (1986).

[41]C.Y. Chu and J.P. Singh, "Mechanical Properties and Microstructure of Si_3N_4-Whisker-Reinforced Si_3N_4-Matrix Composites," *Ceram. Eng. Sci. Proc.*, **11** [7–8] 709–20 (1990).

[42](a) P.F. Becher, M.V. Swain, and M.K. Ferber, "Relation of Transformation Temperature to the Fracture Toughness of Transformation-Toughened Ceramics," *J. Mater. Sci.*, **22** [1] 76–84 (1987). (b) P.F. Becher, "Toughening Behavior in Ceramics Associated with the Transformation of Tetragonal ZrO_2," *Acta Metall.*, **34** [10] 1885–91 (1986).

[43]P.F. Becher, "Toughening Behavior Involving Multiple Mechanisms: Whisker Reinforcement and Zirconia Toughening," *J. Am. Ceram. Soc.*, **70** [9] 651–54 (1987). □

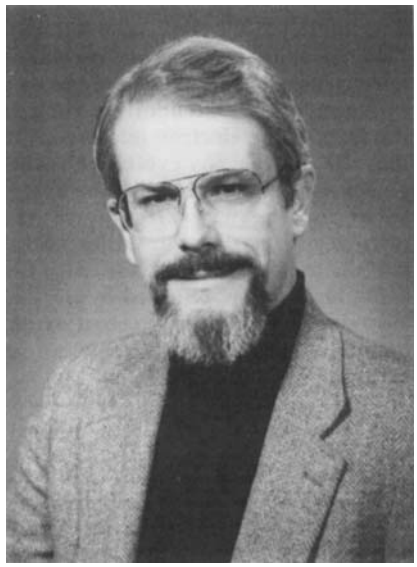

Paul F. Becher is a leader of the Structural Ceramics Group at Oak Ridge National Laboratory (ORNL). He earned his B.Sc. (1963) in metallurgical engineering at the University of Missouri-Rolla and his Ph.D. in ceramic engineering at North Carolina State University. Becher was with the U.S. Naval Research Laboratory and Jet Propulsion Laboratory prior to joining ORNL in 1980. He has authored or coauthored more than 120 technical papers. A Fellow of the American Ceramic Society, Becher has served as chair of the Basic Science Division and currently is Vice President for Programs. In addition to delivering the Sosman Lecture during the 1990 annual meeting, Becher was a member of a team of ORNL authors that received the 1990 Ross Coffin Purdy Award.